

Review Paper: A Study of Monotectic Al-Bi Alloys Rapidly Solidified from Melt

Sanaa Razzaq Abbas¹

Mohammed S. Gumaan²

1. Ministry of Education , Iraq. sanaarazzaq@yahoo.com
2. Biomedical Engineering Department- Faculty of Engineering- University of Science and Technology-Yemen m.gumaan1@gmail.com

Article Information

Submission date: 18 / 9/ 2020

Acceptance date: 13 /10/ 2020

Publication date: 31/ 12/ 2020

Abstract

This paper presents experimental results and theoretical considerations to investigate the effect of rapid cooling from melt on physical properties of Al-Bi alloys. A number of monotectic Al-rich binary alloys having limited solubility in the solid state have been pointed up as desirable for many industrial applications, e.g., self-lubricated bearings, electronic materials, superconductors and optical components. Monotectic alloys undergo an invariant reaction at the monotectic temperature, in which a liquid phase, L_1 , is decomposed into a solid phase, S_1 , and a liquid phase, L_2 . During cooling, the minority liquid phase forms discontinuous and isolate droplets or fibers within the Al-matrix. The competition between the growth of the minority phase and the rate of displacement of the solidification interface will determine if the prevalent morphology will be formed by droplets or fibers. Chill-block melt spinning technique was used to examine the possibility of casting Al-Bi monotectic alloys with possible homogeneous microstructure. The resulting microstructure was analysed by scanning electron microscopy and X-ray diffraction. The electrical resistivity, thermal parameters, internal friction, thermal diffusivity, elastic moduli and hardness of the melt-spun ribbons have been investigated as a function of composition. The results reveal that several combinations of strength, hardness, enthalpy, entropy change, resistivity and internal friction can be generated from the alloys to meet the needs of antifriction applications.

Keywords: Melt-spinning technique, X-ray diffraction, crystal size and lattice distortions, Resistivity, Elastic moduli, internal friction, and micro-hardness

Introduction

Melt-spinning way was used to form the templates or ingots of rapidly solidified Al-Bi alloys. Rapid solidification process effects were observed on the properties of physical state and microstructure of Al-Bi bearing alloys. On the other hand, the primary aluminum is used for the target of the metallurgical industries. One study showed that aluminum alloys characteristics depend on the structure of metallurgical industries, which depends on many points such as the arrangement or the components, postsolidification thermal, deformation processing and solidification processes [1, 2, 3]. There are huge applications as significant functional and structural substances of Aluminum base immiscible monotectic alloys. Depending on their load-bearing ability structural materials were chosen, the strength of response to electrical, optical, thermal and chemical motivations, magnetic determine the functional materials, and they are related the crystallographic and electronic structures of the crystal [4]. Alloys, for

instance, Al–Pb or Al–Bi are possible tools for developed status in automotive uses and these alloys have a miscibility gap in the liquid form. Usually, combined metals in solid metal milieu such as Cu, Al or Al–Si are coming from soft metal components such as Pb, Sn, In and Bi, that process of combination above is for the production of alloys to use them with a hugely lesser contact coefficient and an extremely smaller resistance in comparison with the typical alloys which that in engines of cars: lead and bronze [5]. Because of the huge difference in density in comparison in the two status of the liquid phase, some immiscible alloys cannot be cast using classical casting ways [5, 6]. As a significant method to study new solidification theories, their method has become one of focus in materials science and engineering investigation [7]. Because of that previously, Rapid solidification is an interested search for many researchers. For the production of new structures and improved properties in many of metallic alloys, there is interesting in using rapid solidification processing by the scientific and technological, with cooling rates during solidification of $>10^5 \text{ K s}^{-1}$. Despite of the fact for benefits of the using of Al–Bi monotectic alloys in tribological uses, no studies have been carried out to examine the interaction between structure and physical manners of these monotectic alloys using melt-spinning. Therefore, the present study has been planned to investigate that details and interactions which have been mentioned previously by using melt-spinning. On the other hand, the present study goals to provide a better knowledge on the structure and properties of Al–Bi immiscible alloys created by chill-block melt-spinning [8] to examine the composition with evolution of structure.

Materials and methods

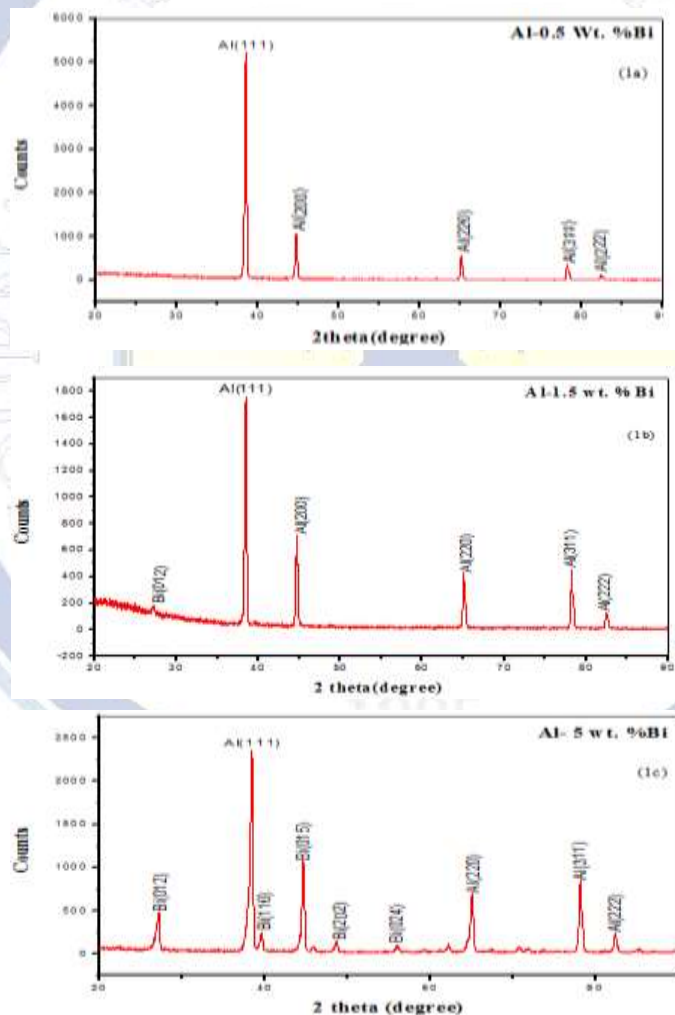
Al and Bi fragments are the tools used in this search, the purity which started by it in the study was better than 99.99 %. The production of the group of Al-(x) wt. % Bi (where $x = 0.5, 1.5, 5, 8, 10, 15, 20, 25, 34, 88$ and $92 \text{ wt. } \%$), was produced by a single aluminum roller coated with copper (200mm in diameter) melt-spinning technique [8]. Amounts of metals which are required to be used in the study were weighed out and heated up to melting in a porcelain container. The temperature which was required for the melting of metals was about $500 \text{ }^\circ\text{C}$ and done in air atmosphere. The linear speed of 30.4 ms^{-1} which matches to the copper wheel speed which was stable at 2900 r.p.m., in the purpose of production ribbons with width of 4mm and $60 \mu\text{m}$ in thickness. Shimadzu x-ray diffractometer was used for the analysis of X-ray diffraction, by using radiation of $\text{Cu } \alpha$ ($\lambda=1.5406 \text{ \AA}$) with Ni-filter. Scanning electron microscope (SEM) of type (JEOL JSM-6510LV, Japan) was purchased for the purpose of analysis the microstructure; (SEM) has high resolution 3nm which operates at 30 Kv. The analysis of differential thermal (DTA) was done by using (SDT Q600, USA), this analysis was applied with a heat rate $10^\circ\text{C min}^{-1}$. the double-bridge techniques was used to determine temperature requirement of resistivity [9]. Step-down transformer linked to a created temperature control was used to fix the difference of temperature during the resistance temperature investigation. At 5 K min^{-1} the heating was maintained stable along with the investigations [10]. In air atmosphere with an adjusted dynamic resonance way, the elastic moduli, the internal friction and the thermal diffusivity of melt-spun ribbons were examined [11]. Digital Vickers microhardness tester (model FM-7) was used to determine the solidity of the melt-spun

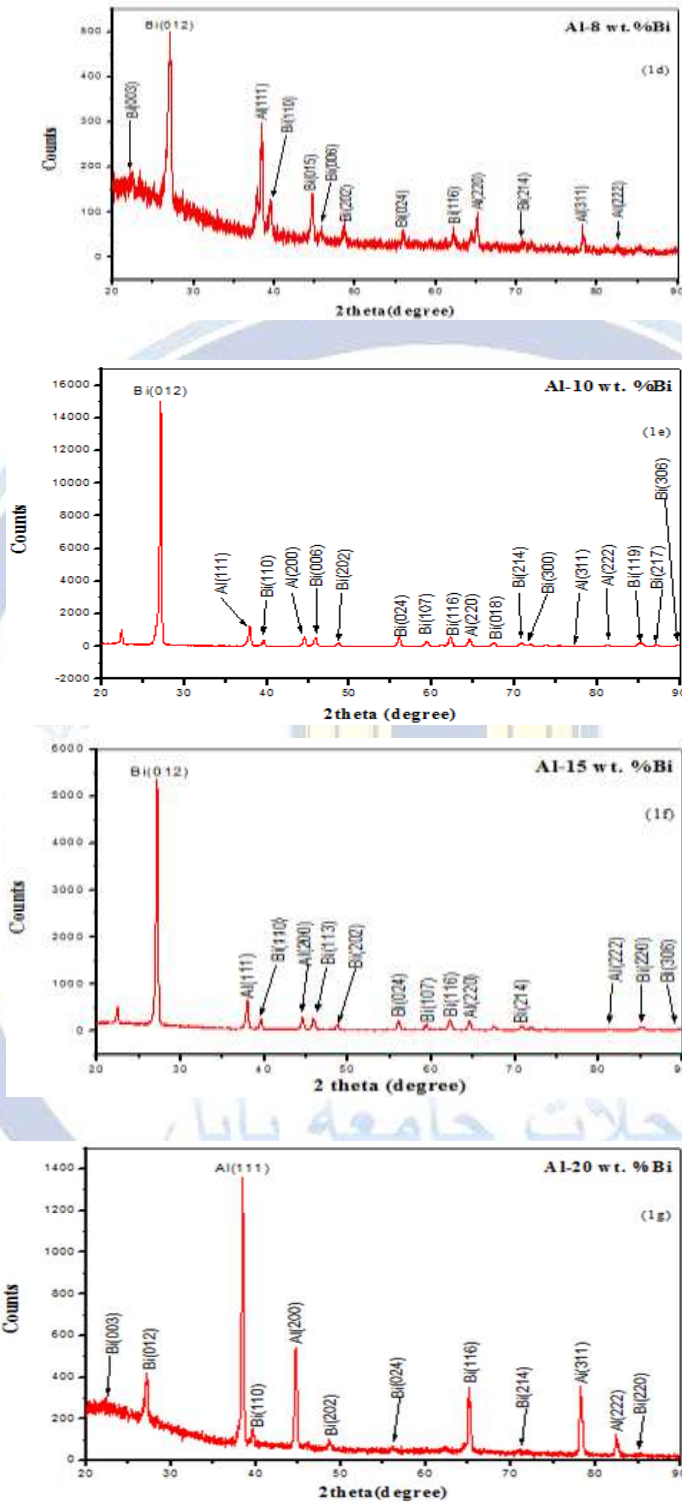
ribbons, Vickers diamond pyramid was used to apply a load of 10gf for 5sec [12]. Because of the existence of more phases, in each sample more than fifteen indents to get out any hardness difference, so that the average value HV would be gained in melt-spun Al-(x) wt. % Bi (where $x = 0.5, 1.5, 5, 8, 10, 15, 20, 25, 34, 88$ and 92 wt. %) ribbons.

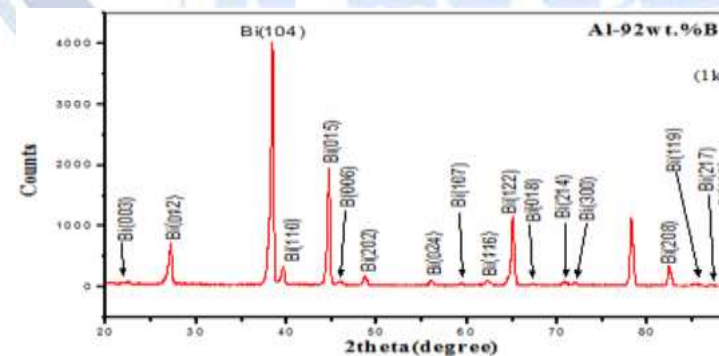
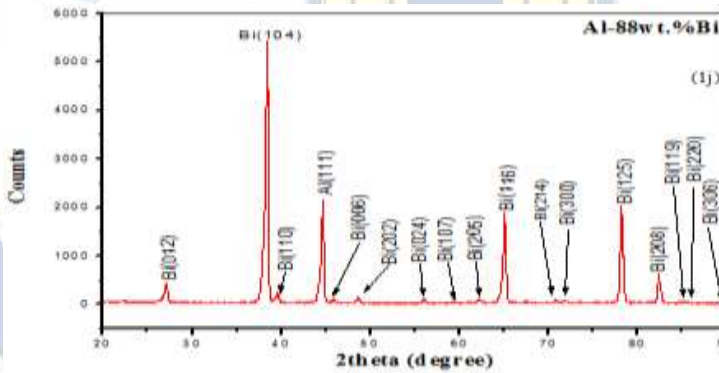
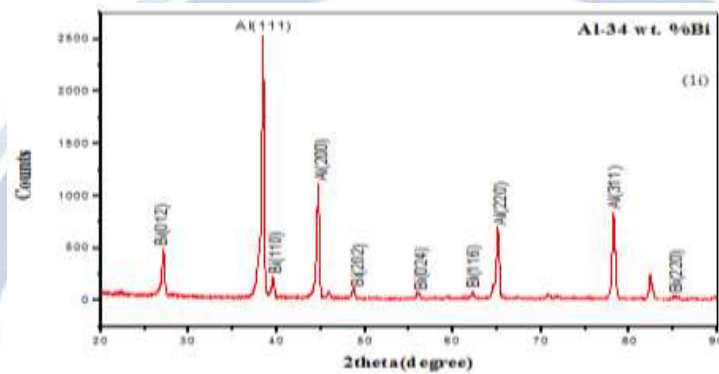
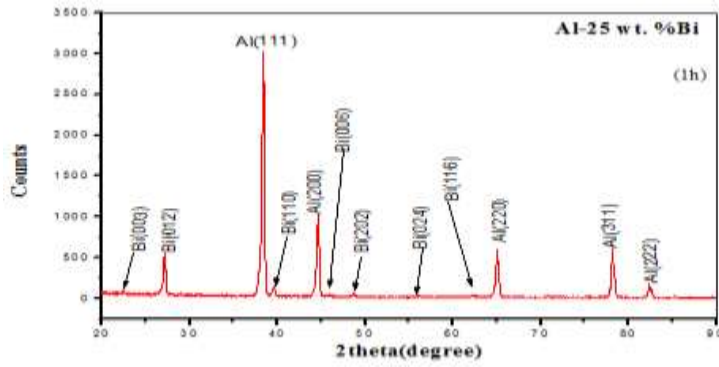
Results and discussions

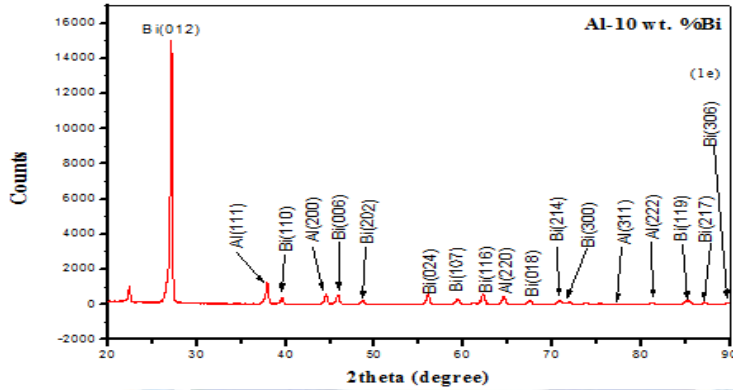
1. Structural analysis

Pol Duwez *et al*, was first who pointed out about the rapid slaking of metallic alloys from melt [13, 14]. The tops or peaks of bismuth and aluminum were only showed by the method of X-ray of the melt-spun ribbons. Due to scientific problem in density, electronegativity, atomic radius and usual valance in aluminum and bismuth, such as that shown in (Fig. 1), so the phase diagram of Al-Bi displayed that is no solid solubility because of those problems above.



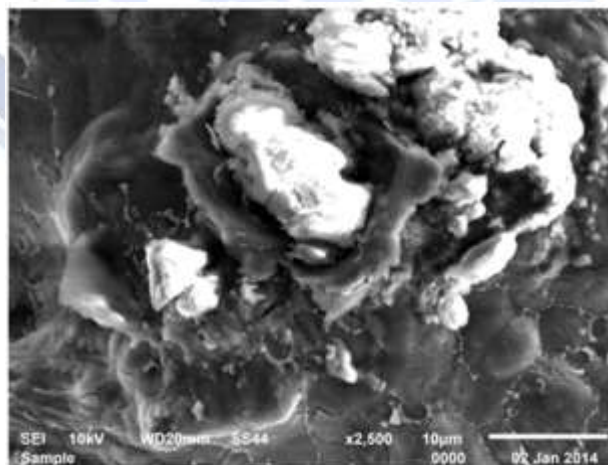
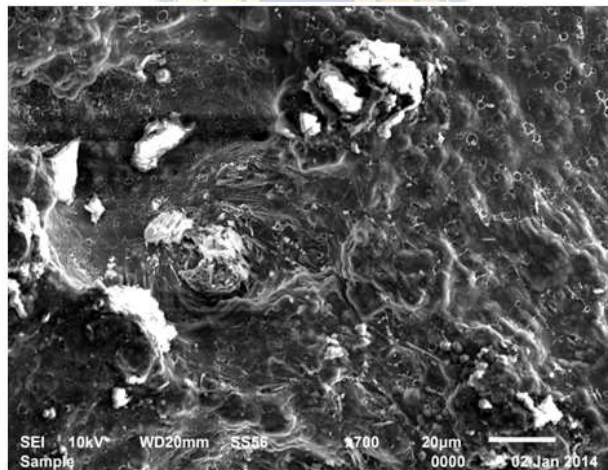






1- a, b, c, d, e, f, g, h, I, j and k): X-ray diffraction pattern melt-spun ribbons.

Illustrates the existence of spread particles in the aluminum matrix which presented by scanning electron microscopy (SEM). It displays a typical SEM micrograph of the melt-spun ribbons of (grey) showing a fine distribution of the bismuth particles in the aluminum matrix (dark). Spreading of fine submicron particles was illustrated by the microstructure.



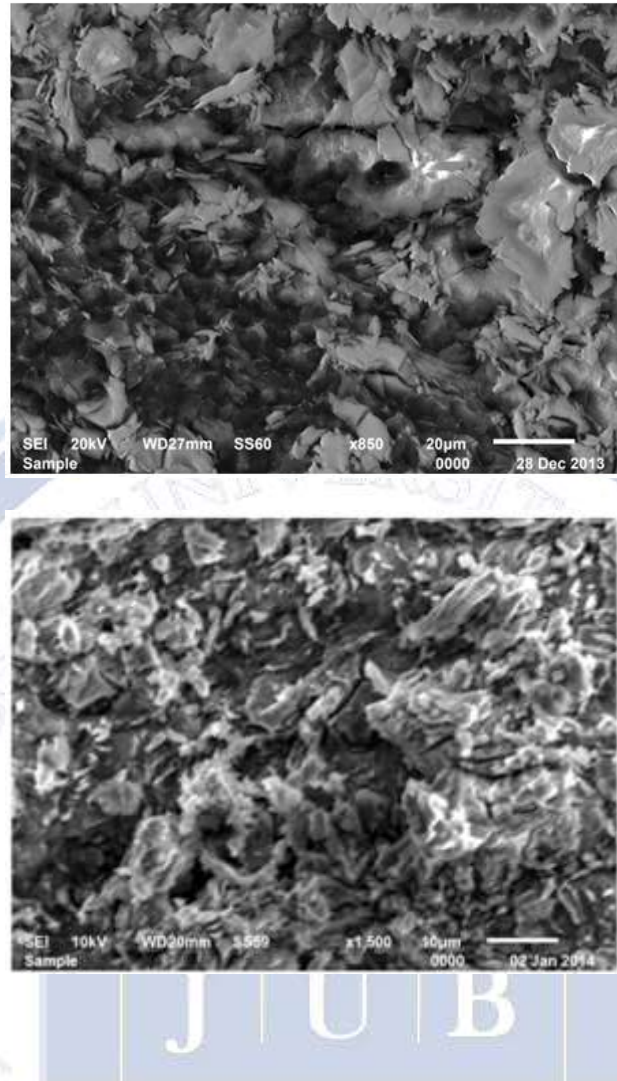


Fig. 2. SEM micrograph of the melt-spun ribbons

The data of lattice parameter Measurement of Al-(x) wt. % Bi (where $x = 0.5, 1.5, 5, 8, 10, 15, 20, 25, 34, 88$ and 92 wt. %) ribbons. The changes which are very small in interplanar spacing as the solute diverse of concentrations that made melt-spun ribbons are hard. As shown in table (I) below. The data of the lattice parameter of Al-(x) wt. % Bi (where $x = 0.5, 1.5, 5, 8, 10, 15, 20, 25, 34, 88$ and 92 wt. %) ribbons.

Table (I)

| Melt-spun ribbons | Al phase | | |
|-------------------|----------|------------------------------|--------------|
| | a (Å) | cell volume (Å) ³ | crystal size |
| Al-0.5 wt. %Bi | 4.0558 | 66.7159 | 26.174 |
| Al-1.5 wt. %Bi | 4.0579 | 66.8196 | 285.317 |
| Al-5 wt. %Bi | 4.0579 | 66.8196 | 255.307 |
| Al-8 wt. %Bi | 4.0512 | 66.4891 | 298.403 |
| Al-10 wt. %Bi | 4.0551 | 66.6764 | 236.982 |
| Al-15 wt. %Bi | 4.0506 | 66.4596 | 251.878 |
| Al-20 wt. %Bi | 4.0577 | 66.8097 | 249.490 |
| Al-25 wt. %Bi | 4.0569 | 66.7702 | 236.089 |
| Al-34 wt. %Bi | 4.0543 | 66.6419 | 207.560 |
| Al-88 wt. %Bi | 4.0574 | 66.7949 | |
| Al-92 wt. %Bi | | | |

Bravais lattice of any crystal is determining the number of atoms per unit cell. Based on a face centered cubic lattice such as in our case, the number of atoms per unit cell in a crystal should be a multiple by 4. The existence of a cell having a non-integer number of atoms also was found in the practice, but there is point defects which is usually in this this type of melt-spun ribbons and is called a nonstoichiometric melt-spun ribbons [14,15], as shown clearly in table (II).

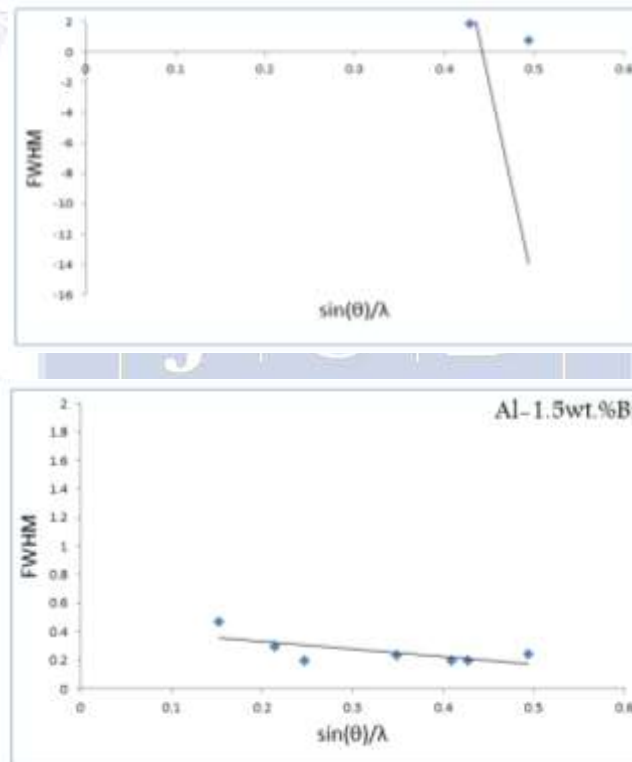
Table (II)

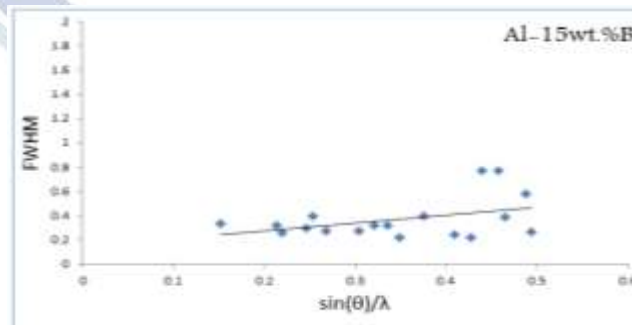
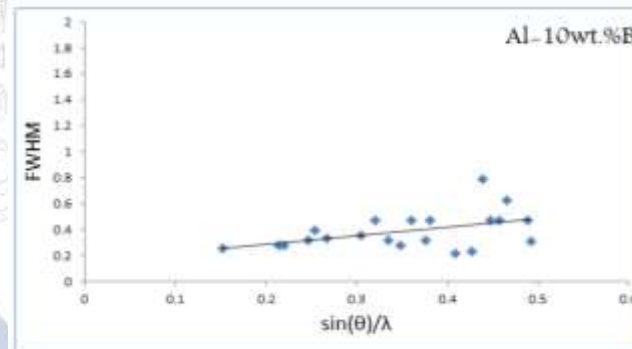
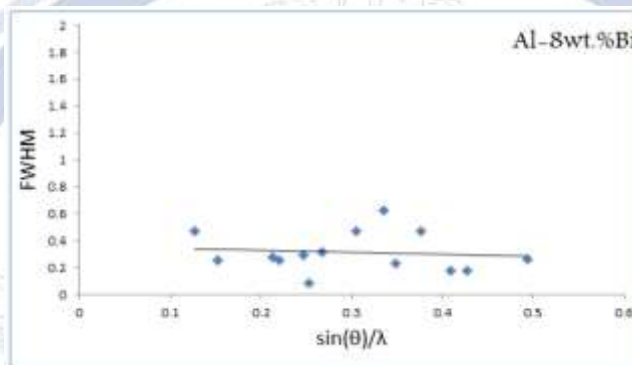
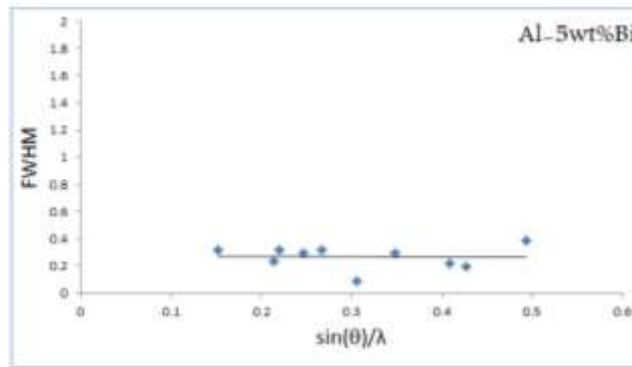
| Melt-spun ribbons | Al phase | |
|-------------------|----------------------------|------------------------------|
| | No. of atoms per unit cell | Density (g/cm ³) |
| Al pure | 4 | 2.68 |
| Al-0.5 wt. %Bi | 3.859 | 2.75 |
| Al-1.5 wt. %Bi | 3.729 | 2.86 |
| Al-5 wt. %Bi | 3.195 | 2.99 |
| Al-8 wt. %Bi | 2.953 | 3.02 |
| Al-10 wt. %Bi | 2.688 | 3.28 |
| Al-15 wt. %Bi | 2.421 | 3.43 |
| Al-20 wt. %Bi | 2.178 | |
| Al-25 wt. %Bi | | |
| Al-34 wt. %Bi | | |
| Al-88 wt. %Bi | | |
| Al-92 wt. %Bi | | |

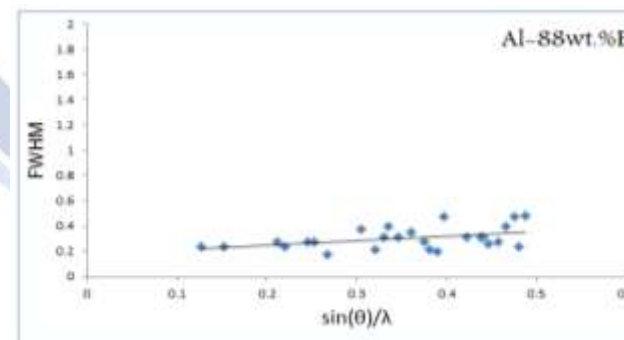
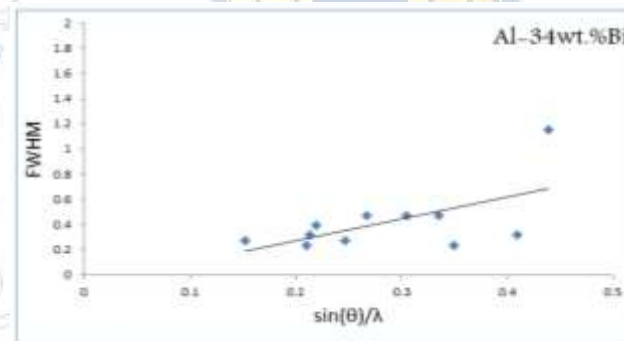
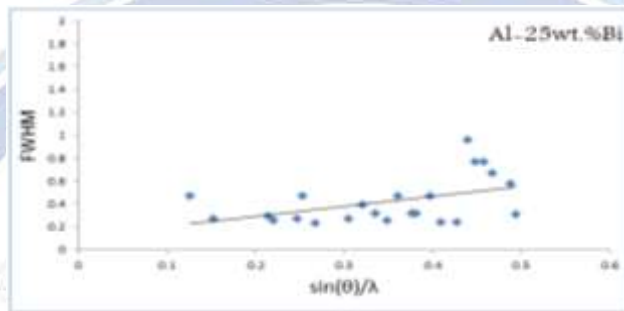
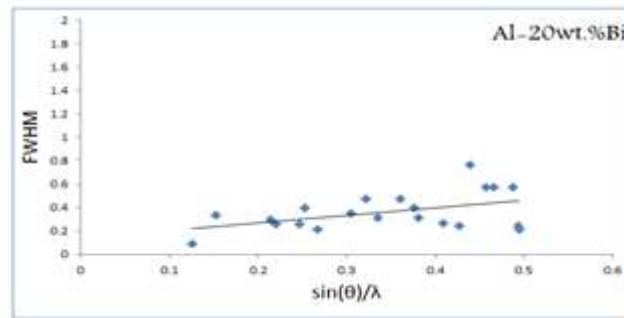
At a particular 2θ angle the increasing observation of diffraction at the top can be noticed by its full width at half maximum FWHM value at that angle. The FWHM values may not be exact enough to be involved in the study to create the instrumental FWHM curve, that because of these values are valued from top areas. On the other hand, lattice strains alone, or lattice strain and small particle are leading to that broadening which is recommended by other study [16]. G. K. Williamson and W. H. Hall, stated that the changes in the intensity spreading of diffracted X-rays are resulted by the rapid solidification from melt of monotectic alloys [17]. To provide information about the size of coherent zones (crystallite size D_{eff}) and local lattice distortion $\langle \Sigma^2 \rangle$ in aluminum phases was used line widths B, both FWHM and integral, in a Williamson- Hall plot [18] as displayed in (Fig. 3).

$$B = \frac{1}{D_{eff}} + 5 \langle \varepsilon^2 \rangle^{1/2} \sin \frac{\theta}{\lambda} \dots \dots \dots (1)$$

The $1/D_{eff}$ and $5 \langle \Sigma^2 \rangle^{1/2}$ parameters are given in Table (III).







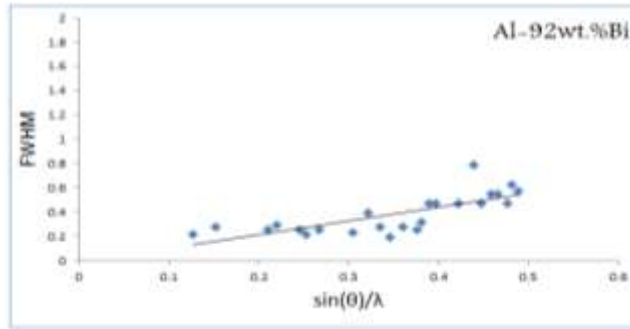


Fig. 3. William-Hall plot of FWHM values for Al-Bi melt-spun ribbons.

Table (III)

| Melt-spun ribbons | Al phase | | |
|-------------------|------------------|--|--|
| | crystal size (Å) | $1/D_{eff} (\text{Å})^{-1} \times 10^{-3}$ | $5\langle \epsilon \rangle^2 \times 10^{-3}$ |
| Al pure | 26.174 | 269 | 115 |
| Al-0.5 wt. %Bi | 285.317 | 2.34 | 0.961 |
| Al-1.5 wt. %Bi | 255.307 | 2.61 | 1.08 |
| Al-5 wt. %Bi | 298.403 | 2.27 | 9.36 |
| Al-8 wt. %Bi | 236.982 | 2.80 | 1.14 |
| Al-10 wt. %Bi | 251.878 | 2.67 | 1.10 |
| Al-15 wt. %Bi | 249.490 | 2.66 | 1.11 |
| Al-20 wt. %Bi | 236.089 | 2.77 | 1.13 |
| Al-25 wt. %Bi | 207.560 | 3.13 | 1.26 |
| Al-34 wt. %Bi | | | |
| Al-88 wt. %Bi | | | |
| Al-92 wt. %Bi | | | |

In order to create a conclusion to a good state of crystallization. Hence the aluminum matrix is lesser disorder than the bismuth phase for all compositions assistant the stacking-fault separation origin of the bismuth lattice. In a F.C.C lattice, what types of assembling are possible? Moreover, let us consider for the purpose of easiness a close-packed lattice made up of spheres of the same size as illustrated in (Fig 4). If there is already a layer, the spheres centers are determined by A a additional layer can be located above either of two groups of hollows in the first layers. The spheres centers are in order over points A, B, C, A, B, C,....., if the layers are following each other, then a close-packed cubic (face-centered) lattice is gained, the close-packed layers forming its {111} planes [19].

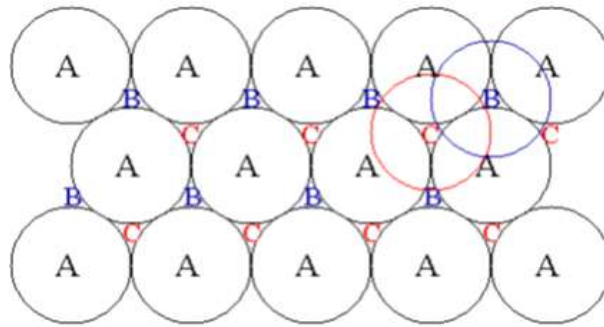


Fig. 4. Close packed layer (111) plane of the FCC lattice

Therefore, as a result of some effect the regular assembling sequence becomes damaged, and a stacking-fault is formed for instance in the following way which it may simply happens:

↓
 ... ABC ABABC ABC ...

A stacking-fault was found which is showed by arrow position. If there more than one probability for the preparation of the atomic layers the stacking faults will be formed. That is because of introducing the stacking operator could not come after two layers of identical character [19]. The number of possibility of stacking orders will be increased if the structure is more complicated. The boundaries of the anti-phase domains are also stacking-faults in ordered alloys.

1. Resistivity and thermal conductivity

Alloys electrical conductivity can be evaluated by using Electrical resistivity; and it became very interested by the researchers. In this study, the creation of ordered alloys was due to the resistivity is measured at about room temperature. The state of deformation and the amount of alloying present are responsible of the rising of rate of electrical resistivity of a metal with temperature. In fact, the real reason of resistivity must therefore be required in deviations from the periodicity of the potential which the electron is moving on it. The modern theory of conductivity was based on this idea. The possible causes of deviations from the periodicity of the potential causing resistivity maybe: (1) boundaries (2) lattice defects (3) lattice vibrations (4) foreign impurity atoms. According to the quantum theory, the electrical conductivity σ value is:

$$\sigma = \frac{ne^2\tau_f}{m_e} \dots\dots\dots (2)$$

The electron crash time value at Fermi surface, τ_f could be directly calculated by using equation (2) provided

| Melt-spun ribbons | $\sigma(\Omega^{-1}.m^{-1}) \times 10^5$ | Electron density (m^3) $\times 10^{27}$ | Fermi wave Vector (m^{-1}) $\times 10^{+9}$ | Fermi energy ($E_f(T)ev$) | Fermi velocity (V_f) $\times 10^5$ | Electron mobility μ ($m^2.v1.s^{-1}$) $\times 10^{-3}$ | Collision time T $\times 10^{-14}$ |
|-------------------|--|---|---|-----------------------------|--|--|------------------------------------|
| Al-0.5 wt. %Bi | 13.7 | 4.857 | 5.239 | 1.046E+00 | 6.068 | 1.7604 | 1.001 |
| Al-1.5 wt. %Bi | 1.695 | 0.6010 | 2.611 | 0.2597E+00 | 3.024 | 1.7604 | 1.001 |
| Al-5 wt. %Bi | 14.49 | 5.139 | 5.339 | 1.086E+00 | 6.183 | 1.7604 | 1.001 |
| Al-8 wt. %Bi | 9.661 | 3.426 | 4.664 | 0.8287E+00 | 5.402 | 1.7604 | 1.001 |
| Al-10 wt. %Bi | 9.202 | 3.263 | 4.588 | 0.8022E+00 | 5.315 | 1.7604 | 1.001 |
| Al-15 wt. %Bi | 7.880 | 2.794 | 4.357 | 0.7234E+00 | 5.047 | 1.7604 | 1.001 |
| Al-20 wt. %Bi | 14.04 | 4.980 | 5.283 | 1.063E+00 | 6.119 | 1.7604 | 1.001 |
| Al-25 wt. %Bi | | | | | | | |
| Al-34 wt. %Bi | | | | | | | |
| Al-88 wt. %Bi | | | | | | | |
| Al-92 wt. %Bi | | | | | | | |

the conductivity is known [20]. A list of the electrical conductivities and other transport parameters of Al-(x) wt. % Bi (where x = 0.5, 1.5, 5, 8, 10, 15, 20, 25, 34, 88 and 92 wt. %) melt-spun ribbons are listed on the Table (IV). On the other hand, values of the equivalent Fermi temperature, Fermi velocities V_F and Fermi wave vector, K_F , are given too. The electrical conduction procedure allows us to calculate the density of states at the Fermi surface F_S , $g(E_F)$ within the framework of band theory which is in general another significant idea of the electrical conduction method [21]. Finally, this makes the following expression for the electrical conductivity:

$$\sigma = \frac{1}{3} e^2 V_F^2 \tau_F g(E_F) \dots\dots\dots (3)$$

It is detected that the states density at the Fermi surface F_S , $g(E_F)$ responsible for the situation of the electrical conductivity. The states density for the melt-spun ribbons of Al-(x) wt. % Bi (where x = 0.5, 1.5, 5, 8, 10, 15, 20, 25, 34, 88 and 92 wt. %) were stated in Table (V), showing the Fermi level position for rapidly quenched ribbons. The changes of thermal conductivity are almost same as was created for the electrical conductivity. Between the electrical and thermal conductivities of the alloy there is a distinctive and certain relationship; although the Weidman-Franz ratio does not hold [22]. In the results found that the values of the thermal conductivity of the Al-(x) wt. % Bi (where x = 0.5, 1.5, 5, 8, 10, 15, 20, 25, 34, 88 and 92 wt. %) melt-spun ribbons is stated in Table (VI).

Table(V)

| Melt-spun ribbons | Fermi energy (E) (ev) | $g(E_f) \times 10^{46}$ |
|-------------------|-----------------------|-------------------------|
| Al-0.5 wt. %Bi | 0.1046E+01 | 4.348 |
| Al-1.5 wt. %Bi | 2.597E+01 | 2.167 |
| Al-5 wt. %Bi | 0.1086E+01 | 4.431 |
| Al-8 wt. %Bi | 8.287E+01 | 3.871 |
| Al-10 wt. %Bi | 8.022E+01 | 3.808 |
| Al-15 wt. %Bi | 7.234E+01 | 3.616 |
| Al-20 wt. %Bi | 0.1063E+01 | 4.385 |
| Al-25 wt. %Bi | | |
| Al-34 wt. %Bi | | |
| Al-88 wt. %Bi | | |
| Al-92 wt. %Bi | | |

Table(V1)

| Melt-spun ribbons | Thermal conductivity(K) (w.m-1.k-1) | Electron specific heat(Ce)(J/kg-1 .k-1) |
|-------------------|-------------------------------------|---|
| Al-0.5 wt. %Bi | 10.11 | 1.014 |
| Al-1.5 wt. %Bi | 1.251 | 4.085 |
| Al-5 wt. %Bi | 10.7 | 0.976 |
| Al-8 wt. %Bi | 7.13 | 1.280 |
| Al-10 wt. %Bi | 6.79 | 1.322 |
| Al-15 wt. %Bi | 5.815 | 1.466 |
| Al-20 wt. %Bi | 10.36 | 0.997 |
| Al-25 wt. %Bi | | |
| Al-34 wt. %Bi | | |
| Al-88 wt. %Bi | | |
| Al-92 wt. %Bi | | |

3-Elastic constant

Generally, the components of Polycrystalline solids are randomly oriented crystallites display or show manner of the quasi-isotropic elastic. The deficiency free materials magnitude is a function of the magnitude of the atomic bonds rigidity. In fact, polycrystalline materials, other factors, for instance, porosity, texture, levels of impurities and components of alloying, intergranular phases, etc could effect the elastic constants magnitude. Due to the simplicity of sample preparation a benefit over static technique can be given by Dynamic techniques, extensive diversity of sample shapes and sizes, huge accuracy and measurement over a varied temperature range, moreover, the low-level alternating stress does not fill or expand anelastic procedures for instance, creep or elastic hysteresis [23]. The elastic constant such as young's modulus E, shear modulus G, bulk modulus B and poisson's ratio ν for isotropic polycrystalline melt-spun ribbons could be evaluated or calculated from equations below:

$$E = \frac{38.32\rho l^4 f^2}{t^2} \dots\dots\dots (4)$$

$$G = \frac{E}{2(1+\nu)} \dots\dots\dots (5)$$

$$B = \frac{E}{3(1-2\nu)} \dots\dots\dots (6)$$

Table (VII) shows the young's modulus, the shear modulus, the bulk modulus and the poissons ratio for Al-(x) wt. % Bi (where x = 0.5, 1.5, 5, 8, 10, 15, 20, 25, 34, 88 and 92 wt. %) melt spun ribbons.

Table (VII)

| Melt-spun ribbons | Young's modulus (GPa) | Shear modulus (GPa) | Bulk modulus (GPa) | Poisson,s ratio |
|-------------------|-----------------------|---------------------|--------------------|-----------------|
| Al-0.5 wt. %Bi | 29.66 | 10.99 | 32.93 | 0.3499 |
| Al-1.5 wt. %Bi | 29.21 | 10.82 | 32.39 | 0.3497 |
| Al-5 wt. %Bi | 22.16 | 8.21 | 24.46 | 0.349 |
| Al-8 wt. %Bi | 20.76 | 7.70 | 22.82 | 0.3484 |
| Al-10 wt. %Bi | 20.11 | 7.46 | 22.05 | 0.348 |
| Al-15 wt. %Bi | 19.87 | 7.37 | 21.64 | 0.347 |
| Al-20 wt. %Bi | 18.96 | 7.04 | 20.52 | 0.346 |
| Al-25 wt. %Bi | | | | |
| Al-34 wt. %Bi | | | | |
| Al-88 wt. %Bi | | | | |
| Al-92 wt. %Bi | | | | |

In the limit which displayed by data that pointed out that are almost the same up to the 1wt% Bi, Young’s modulus is not sensitive to composition in that ratio above. But, by elevation of the content of bismuth there is more sensitive to composition. Moreover, Table (VII) states the influence of elevation content of bismuth on elastic stiffness which indicates that averages of the fractional change for elastic stiffness is at about 54%. Itseems that the incremental reduce upon additions of bismuth is about the same for all elastic modulus.

Ledbetter [24] and Gorecki [25] stated in a study the base of theoretical part for the experimental relationship between young's modulus E and the shear modulus G and this has been detected for a long time ago

$$G/E \approx 365 \dots\dots\dots (7)$$

Thus, if we consider between young's modulus there is the well-known relation, the shear modulus and the bulk modulus:

$$G/E = (3+G/B)/9 \dots\dots\dots (8)$$

The main goal of this part of the study is to find out the logicity of relationship (8), for typical F.C.C structures by detection for experimental relationships for the ratios G/E, G/B, and E/B for each melt-spun ribbon in separation way. Table (VIII) displayed the results of statistical analysis of the G, E and B for melt-spun ribbons relationships

Table (VIII)

| Melt-spun ribbons | G/E | G/B | E/B |
|-------------------|-------|-------|-------|
| Al-0.5 wt. %Bi | 0.370 | 0.333 | 0.900 |
| Al-1.5 wt. %Bi | 0.370 | 0.334 | 0.901 |
| Al-5 wt. %Bi | 0.370 | 0.335 | 0.905 |
| Al-8 wt. %Bi | 0.370 | 0.337 | 0.909 |
| Al-10 wt. %Bi | 0.370 | 0.338 | 0.912 |
| Al-15 wt. %Bi | 0.370 | 0.340 | 0.918 |
| Al-20 wt. %Bi | 0.371 | 0.343 | 0.923 |
| Al-25 wt. %Bi | | | |
| Al-34 wt. %Bi | | | |
| Al-88 wt. %Bi | | | |
| Al-92 wt. %Bi | | | |

4-Internal friction

The internal friction Q^{-1} is considered as a significant feature which is related indirectly way to their elastic properties. Because of the same method (dynamic resonance technique) is detailing in the part of the experimental method could be applied to evaluate the internal friction Q^{-1} . In general, the way that used for the measurement of internal friction of quenched ribbons is divided into the following types: Free-vibration method –direct observation of stress-strain curves –wave propagation method, and forced-vibration method. The influence of impurity content on the elastic characteristics was easy to detect it with these methods which have been mentioned above. Thus, the measurements of internal friction had are very useful and promising for learning Al-Bi quenched ribbons will behave, to small changes in the mechanical state of quenched ribbons, the internal friction is capable to respond . The composition of anelastic (the time-dependent elastic behavior) was found is small and insignificant. The internal friction is gained by equation below [26].

$$Q^{-1} = 0.5773 \frac{\Delta f}{f} \dots\dots\dots (9)$$

Where f is a critical frequency of quenched ribbons. Table (IX) presents the internal friction for Al-(x) wt. % Bi (where x = 0.5, 1.5, 5, 8, 10, 15, 20, 25, 34, 88 and 92 wt. %) melt-spun ribbons.

Table (IX)

| Melt-spun ribbons | Internal friction Q^{-1} |
|-------------------|----------------------------|
| Al-0.5 wt. %Bi | 0.0177 |
| Al-1.5 wt. %Bi | 0.0211 |
| Al-5 wt. %Bi | 0.0218 |
| Al-8 wt. %Bi | 0.0188 |
| Al-10 wt. %Bi | 0.0197 |
| Al-15 wt. %Bi | 0.036 |
| Al-20 wt. %Bi | 0.0251 |
| Al-25 wt. %Bi | |
| Al-34 wt. %Bi | |
| Al-88 wt. %Bi | |
| Al-92 wt. %Bi | |

The internal friction Q^{-1} is more sensitive than the elastic moduli to the phase changes happening in the quenched ribbons and that was shown clearly by Table (IX) [27].

5-Thermal diffusivity

Measuring the thermal diffusivity of quenched of Al-(x) wt.% Bi (where x = 0.5, 1.5, 5, 8, 10, 15, 20, 25, 34, 88 and 92 wt. %) ribbons can be achieved using dynamic resonance method. At the frequency f, where reduction of the top is happens, the thermal diffusivity D could be directly gained from the relation:

$$D = \frac{2t^2f}{\pi} \dots\dots\dots (10)$$

Where t is present the thickness of quenched ribbons. The thermal diffusivity for Al-(x) wt. % Bi (where x = 0.5, 1.5, 5, 8, 10, 15, 20, 25, 34, 88 and 92 wt. %) melt-spun ribbons, as these values are displayed in Table (X).

Table (X)

| Melt-spun ribbons | Thermal diffusivity D_{th} (m^2/sec) $\times 10^{-7}$ |
|--------------------------|---|
| Al-0.5 wt. %Bi | 2.105 |
| Al-1.5 wt. %Bi | 1.620 |
| Al-5 wt. %Bi | 2.065 |
| Al-8 wt. %Bi | 1.722 |
| Al-10 wt. %Bi | 1.741 |
| Al-15 wt. %Bi | 2.003 |
| Al-20 wt. %Bi | 1.088 |
| Al-25 wt. %Bi | |
| Al-34 wt. %Bi | |
| Al-88 wt. %Bi | |
| Al-92 wt. %Bi | |

6-Micro-hardness investigations

This part of the study is dealing with micro-hardness measuring which applied on rapidly quenched ribbons of Al-(x) wt.% Bi (where x = 0.5, 1.5, 5, 8, 10, 15, 20, 25, 34, 88 and 92 wt. %) from the melt are displayed in Table (XI).

Table (XI)

| Melt-spun ribbons | HV (MPa) |
|--------------------------|-----------------|
| Al-0.5 wt. %Bi | 384.67 |
| Al-1.5 wt. %Bi | 498.42 |
| Al-5 wt. %Bi | 667.10 |
| Al-8 wt. %Bi | 359.90 |
| Al-10 wt. %Bi | 531.77 |
| Al-15 wt. %Bi | 354.27 |
| Al-20 wt. %Bi | 477.58 |
| Al-25 wt. %Bi | |
| Al-34 wt. %Bi | |
| Al-88 wt. %Bi | |

The recorded assessment of Vickers hardness is a rate value of ten indentations made on each melt-spun ribbon by existence of a10 gf. Load for 5 sec to be used. Dispersion strengthening and solid solution strengthening are leading to elevation of bismuth composition and reducing of the micro-hardness value of Al-Bi ribbons material. The result of the study was found there is a various value of the Hv. But the different of this value is not behaves as a linear in manner. Indentation size effects (ISE) is a term which called for the behavior mentioned above (nonlinear). Basing on the indenter permeation depth, the quality of the ISE behavior can be described [28, 29].

Conclusion

The results of this study proof the efficiency of the melt-spinning technique to produce a regular aluminum monotectic alloys. In both theoretical researches and practical uses there is a significant impact for the monotectic alloy with regularly scatters microstructure. For the production of the electricity contacting tools, self lubricative bearings, this type of alloys or materials could be hugely used in this field. In this study, we detected the structure, electrical resistivity, hardness, and elastic modulus of Al-(x) wt. % Bi (where $x = 0.5, 1.5, 5, 8, 10, 15, 20, 25, 34, 88$ and 92 wt. %) alloys. No intermetallic compounds were found by the results all the phase shows Al and Bi phases, that is presented by the measurements of the X-ray. The elevation of bismuth ratio leads to the changing average crystal size and that is shows clearly the change in the hardness and the elastic modulus of the alloys. The alloy with 5wt. % Bi has great electrical and thermal conductivity, good mechanical features, and enough internal friction. Thus, the Al-8wt. %Bi alloy has bearing properties uses. Compounds made of multicomponent alloys with liquid– liquid miscibility are the attention of basic and applied study on creation of new tools with exceptional functional characteristics.

Recommendation: based on the results gained from this work I would like to recommend that this technique is very effective to produce like these types of the alloys as mentioned previously. On the other hand, I don't like to recommend or suggest using this technique for the production of alloys with more than 25% wt Bi due to in this situation will not produce an alloy. But, if produce the alloy it will be very soft with no harness and cannot carry out any test on this alloy except the X-ray test.

Acknowledgment

It is a great pleasure and honor to express my feelings and thanks to Prof. Dr. **Mustafa Kamal Mohammed Yousef** for his kind and sincere support to achieve this research work. Faculty of Science, Mansoura University, Egypt, is greatly appreciated for the facilities and help which are provided by them.



Conflict of Interests.

There are non-conflicts of interest .

References

- [1] P. Schüler, *DEW-Tech. Ber.* 7 (1967) 5-12.
- [2] K. Rüdinger. "Sounderwerkstoffe für den.
- [3] Korrosion-sschutz", in H. Gräfen (ed.): *Die Praxis des Korrosionsschutzes*, vol. 64, "Kontakt u. Studium Werkstoffe", Expert-Verlag, Grafenau/Württ. 1981, pp. 111-144; 345-347.
- [4] J. L. Murray: *Phase Diagrams of Binary Titanium Alloys*, ASM International, Metals Park, OH, 1990.
- [5] Z. L. Wang and Z. C. Kang, plenum press. New York and London, ISBN-O-306-45651-6, functional and smart materials "structural evolution and structure analysis, (1998).
- [6] Ratke L, Diefenbach S. *Mat Sci Eng* 1995;R15: 263.
- [7] Singh RN, Sommer F. *Rep Prog Phys* 1997; 60:57.
- [8] D.L. Li, G.C. Yang, Y.H. Zhou, *Mater. Sci. Lett.* 11 (1992) 1033.
- [9] Mustafa Kamal and Usama S. Mohamed, *A Review Chill-Block Melt spin Technique, Theoretical and Applications*, eISBN: 978-1- 608005-151-9(2012), Bentham eBooks.
- [10] Y.A.Geller, A. G. Rakhshadt, "Science of Materials" ,Mir publishers,Moscow, 1977,P. 138 .
- [11] Mustafa Kamal, Abu-Baker El-Bediwi and Tarek El-Ashram, *Journal of Materials science in Electronics* 15(2004) 211-217.
- [12] A.M. Shaban and M. Kamal, *Radiation Effects and Defects in Solids* (1995),Vol.133, PP:5-13.
- [13] Mustafa Kamal and Abu-Baker El-Bediwi, *Radiation Effects and Defects in solids* 174(1999)211.
- [14] Pol Duwez, R. H. Willens, and W. Klement Jr., *J. Appl. Phys.* 31, 1136 (1960).
- [15] Pol Duwez, R. H. Willens, and W. Klement Jr., *J. Appl. Phys.* 31, 1137 (1960).
- [16] E.A. Van Arkel, *Physica*, 5(1925) 208.
- [17] G. K. Williamson and W. H. Hall, *Acta metal.* 1, 22-31(1953).
- [18] W. H. Hall and G.K. Williamson, *Proc. Phys. Soc* 64B (1951) 937, 946.
- [19] I. Kovacs and L. Zsoldos, *dislocations and plastic deformation*, International Series of Monographic in natural Philosophy, volume 60(1973)165.
- [20] Mustafa Kamal and Abu-Baker-El-Bediwi, *Journal of Materials science: Material in Electronics* 11(2000)519- 523.
- [21] M.A. Omar, *Elementary solid state physics; principles and Application*, Addison-Wesley publishing company, 1975 PP: 235-238.
- [22] G. E. Doan, *The principles of physical Metallurgy*, McGraw Hill Book Company, INC. (1953) PP: 202-231.
- [23] E. Schreiber, O. L. Anderson, and N. Soga, *Elastic Constants and their Measurements*, McGraw-Hill Book Company (1973) PP: 82-125.
- [24] H. M. Ledbetter, *Material Science and Engineering*, 27(1977) 133.
- [25] T. Gorecki, *Material Science and Engineering*, 43(1980) 225.

